

# Semi-cosmological simulations in a growing dark matter potential

Shashank Dattathri

September 8, 2020

## 1 Theory

According to Diemer 2014, the dark matter potential can be expressed in the form

$$\rho = \rho_{inner} f_{trans} + \rho_{outer} \quad (1)$$

The profile of  $\rho_{inner}$  can be two choices:

**NFW profile:**

This profile has density given by

$$\rho(r) = \frac{\rho_0}{r/R_s (1 + r/R_s)^2} \quad (2)$$

The corresponding potential is

$$\Phi(r) = -\frac{4\pi G \rho_0 R_s^3}{r} \ln(1 + r/R_s) \quad (3)$$

The gravitational acceleration is given by

$$\vec{g} = G \frac{M_{vir}}{\ln(1+c) - \frac{c}{1+c}} \times \frac{\frac{r}{r+R_s} - \ln(1 + r/R_s)}{r^3} \vec{r} \quad (4)$$

where the concentration parameter  $c$  is given by  $R_{vir} = cR_s$ , and the virial mass is  $M_{vir} = \frac{4\pi}{3} R_{vir}^3 200\rho_{crit}$ .

**Einasto profile:**

The density profile is given by (Retana-Montenegro 2012)

$$\rho(r) = \rho_s \exp \left( -d_n \left[ \left( \frac{r}{r_s} \right)^{1/n} - 1 \right] \right) \quad (5)$$

where  $\rho_s = \rho(r_s)$ . It is more convenient to express this as

$$\rho(r) = \rho_0 \exp \left( -\left( \frac{r}{h} \right)^{1/n} \right) \quad (6)$$

where  $\rho_0 = \rho_s e^{d_n}$  and  $h = \frac{r_s}{d_n^{1/n}}$ . Here, the total mass is given by

$$M = 4\pi \rho_0 h^3 n \Gamma(3n) \quad (7)$$

The coefficient  $d_n$  can be expressed as a series expansion:

$$d_n \approx 3n - \frac{1}{3} + \frac{8}{1215n} + \frac{184}{229635n^2} + \frac{1048}{31000725n^3} + O\left(\frac{1}{n^4}\right) \quad (8)$$

The general formula for a potential due to a spherical mass is

$$\Phi(r) = -4\pi G \left[ \frac{1}{r} \int_0^r \rho(r') r'^2 dr' + \int_r^\infty \rho(r') r' dr' \right] \quad (9)$$

For the Einasto profile, we have

$$\Phi(r) = \frac{GM}{hs} \left[ 1 - \frac{\Gamma(3n, s^{1/n})}{\Gamma(3n)} + \frac{s\Gamma(2n, s^{1/n})}{\Gamma(3n)} \right] \quad (10)$$

where  $s = \frac{(d_n)^n r}{r^s}$ .

At small radii, the potential is given by

$$\Phi \approx \Phi_0 - \frac{GM}{h} \frac{s^2}{6n\Gamma(3n)} \quad (11)$$

which is a parabolic potential.

For large radii, the potential resembles a Keplerian potential

$$\Phi(r) \approx \frac{GM}{r} \quad (12)$$

### **Outer profile**

Diemer 2014 takes the outer density profile to be

$$\rho_{outer} = \rho_m \left[ b_e \left( \frac{r}{5R_{200m}} \right)^{-s_e} + 1 \right] \quad (13)$$

$$= a \left( b \left( \frac{r}{r_0} \right)^{-c} + 1 \right) \quad (14)$$

The corresponding potential is

$$\Phi(r) = 4\pi G a \left( b r_0^c \frac{r^{2-c}}{(3-c)(2-c)} + \frac{r^2}{6} \right) \quad (15)$$

The corresponding acceleration is

$$\vec{g} = -a \left( b r_0^c \frac{r^{1-c}}{3-c} + \frac{r}{3} \right) \hat{r} \quad (16)$$

### **Transfer function**

The transfer function  $f_{trans}$  from Diemer's paper has the property of going to 1 at small radii and going to 0 at large radii. They take the function

$$f_{trans} = \left[ 1 + \left( \frac{r}{r_t} \right)^\beta \right]^{-\frac{\gamma}{\beta}} \quad (17)$$

They take  $\beta = 4$  and  $\gamma = 8$ . This function is plotted here This looks like a sigmoid function. While choosing a

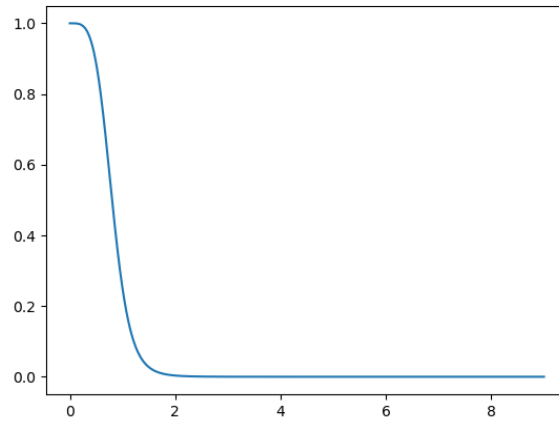


Figure 1:  $f_{trans}$  as a function of  $r/r_t$ .

transfer function  $f(x)$  for the inner to outer transition, it must have the simple property of a sharp transition from 0 to 1 at  $x = r/r_t = 1$ .

### **Constructing the potential**

From equation 1 for the density profile given by Diemer, I construct the corresponding potential by two methods.

Method 1: Direct integration. Given the density profile, we can calculate  $M_{enc}(r) = \int_0^r 4\pi r'^2 \rho(r') dr'$ . From this, the radial derivative of the potential, i.e. the radial acceleration, can be calculated as

$$\frac{d\Phi(r)}{dr} = \frac{GM_{enc}(r)}{r^2} \quad (18)$$

The potential is then calculated by integration of the above equation.

Method 2: Using equation 10. I use the scipy module quadpack to perform the integration, as the potential is continuous and smooth.

### Fitting Potential

The potential is fitted according to

$$\Phi(r) = w_1 \Phi_1 + w_2 \Phi_2 \quad (19)$$

where  $\Phi_1 = \Phi_{NFW}(r)$  (equation 4),  $\Phi_2 = \Phi_{outer}(r)$  (equation 16), and  $w_1$  and  $w_2$  are weight functions.

I take the weight functions as:

$$w_1 = 1 - \left( \frac{1 + \text{erf}(x)}{c_e} \right) \quad w_2 = (1 - w_1^4)^{1/4} \quad (20)$$

where  $\text{erf}(x)$  is the error function,  $x = \log(r/r_t)$ , and  $c_e$  ranges from 5 to 10, dependent on  $\nu$ ,  $R_{200m}$ ,  $s_e$ , and other input parameters.

The results for the fitting potential and the potential constructed by the two methods are shown below. The input parameters are  $\nu = 4$ ,  $b_e = 1.5$ ,  $s_e = 1.5$ ,  $M_{200} = 10^{12} M_\odot$ ,  $z = 0$ .

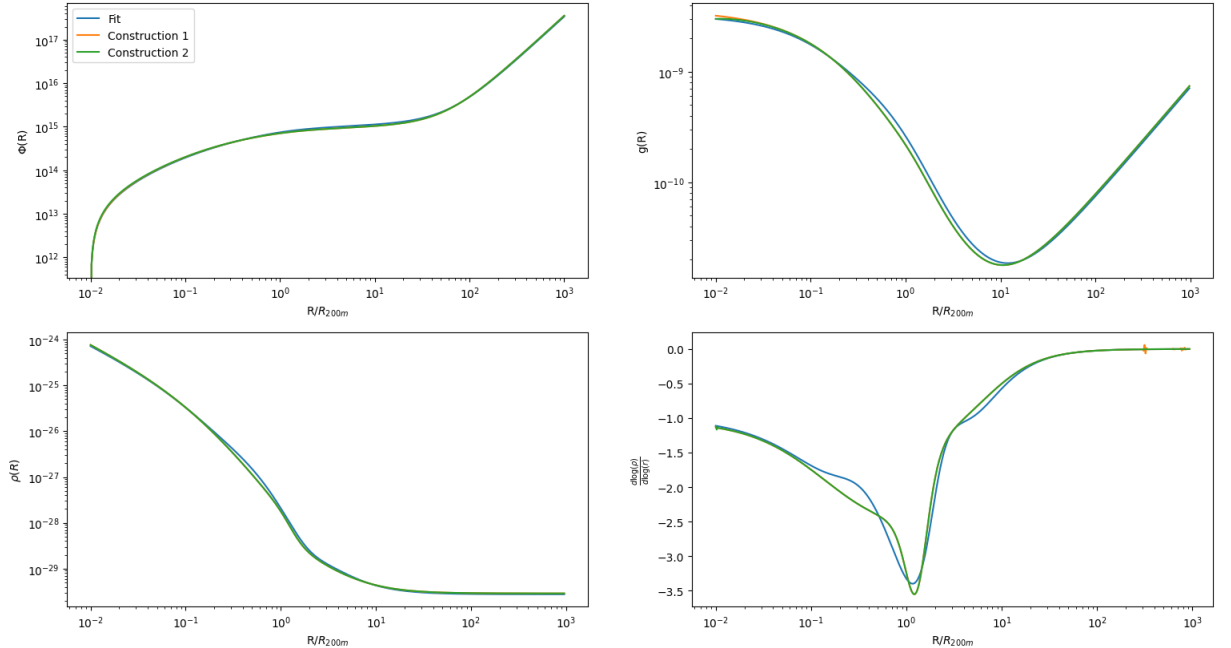


Figure 2: The potential, acceleration, density, and local power law index for the fit and the constructions.

### Evolution of the Halo

The dynamical evolution and growth of the DM halo is given by van den Bosch:

$$\log(M(z)/M_0) = -0.301 \left[ \frac{\log(1+z)}{\log(1+z_f)} \right]^\nu \quad (21)$$

where  $z_f$  is the formation redshift ( $M(z_f) = M_0/2$ ) and  $\nu$  is given by

$$\nu = 1.211 + 1.858 \log(1+z_f) + 0.308 \Omega_\Lambda^2 - 0.032 \log(M_0/10^{11} h^{-1} M_\odot) \quad (22)$$

The concentration parameter of the NFW profile halo evolves as (Zhao et al 2009)

$$c = 4 \left( 1 + \left( \frac{t}{3.75 t_{0.04}} \right)^{8.4} \right)^{1/8} \quad (23)$$

Therefore, the evolution of the DM halo following the NFW profile is completely specified by its present day mass  $M_0$  and its formation redshift  $z_f$ .

Finally, to implement the evolution in PLUTO, the redshift must be converted into lookback time. If the cosmological parameters  $\Omega_m$ ,  $\Omega_\Lambda$ ,  $H_0$  are specified, with the assumption of a flat universe ( $\Omega_m + \Omega_\Lambda = 1$ ), we have

$$t(z) = \frac{1}{H_0} \frac{2}{3\sqrt{\Omega_\Lambda}} \ln \left[ \frac{\sqrt{\Omega_\Lambda(1+z)^{-3}} + \sqrt{\Omega_\Lambda(1+z)^{-3} + \Omega_m}}{\sqrt{\Omega_m}} \right] \quad (24)$$

## 2 Results

The initial conditions are set as

$$\rho_g = 0.2 \times \rho_{DM} \quad v_r = H_0 E_z(z_0) \times r \quad P = K \rho_g^\gamma \quad (25)$$

where  $\rho_{DM}$  is the Diemer density profile and  $K$  is a numerical factor (defined in PPC paper).

I also assume a formation redshift  $z_f = 2$  for all the simulations (this has to be improved). The peak height is set to  $\nu = 4$ .

I run the simulation from  $z = 6$  to  $z = 0$ .

In figure ??, I have plotted the density, pressure, and velocity profiles for  $M_0 = 10^{12} M_\odot$ .

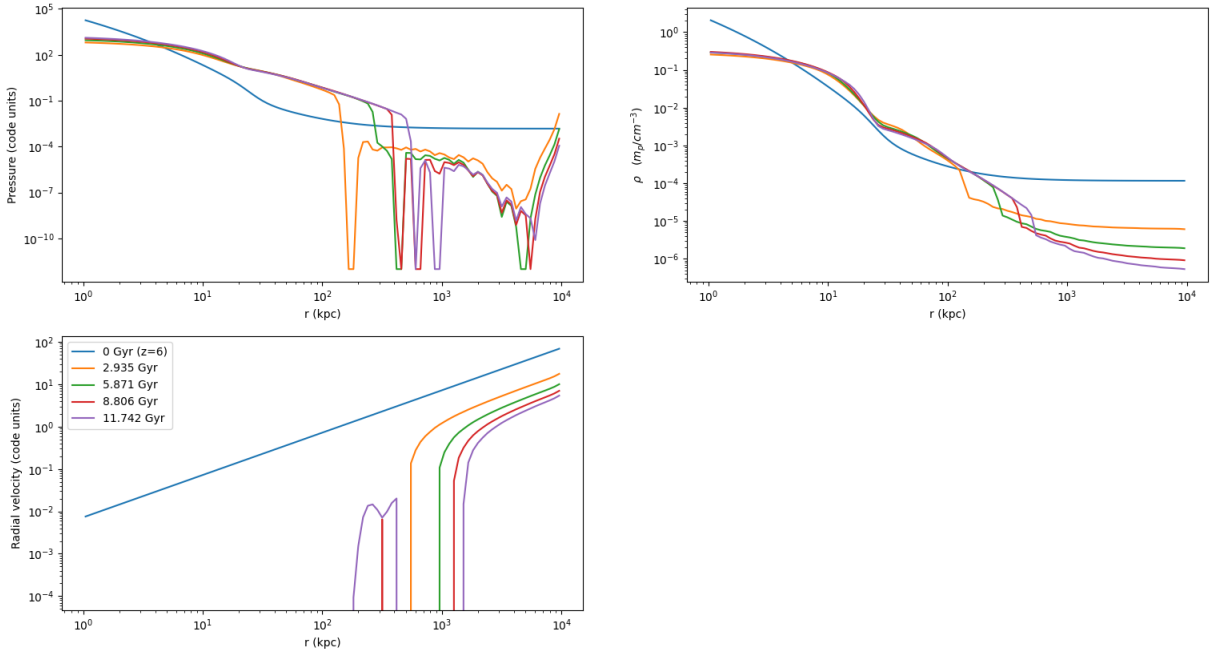


Figure 3: The density, pressure, and velocity profiles for  $M_0 = 10^{12} M_\odot$ .

The effect of dark matter halo can be modelled using either the potential or the acceleration vector. In figure ??, I plot the percentage difference between the two. As they differ by only a few percent (max), I use vector as it has a lesser running time.

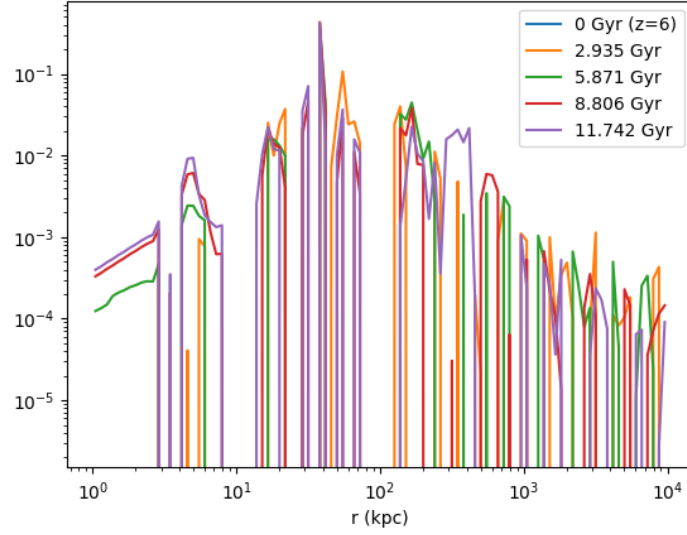


Figure 4: Relative difference between the potential and vector profiles:  $(\rho_p - \rho_v)/\rho_p$

I also plot the baryon fraction withing  $R_{200c}$  as a function of time. The baryon fraction is defined as

$$f_b = \frac{\int_0^{R_{200c}} \rho_g r^2}{\int_0^{R_{200c}} \rho_{DM} r^2 + \int_0^{R_{200c}} \rho_g r^2} \quad (26)$$

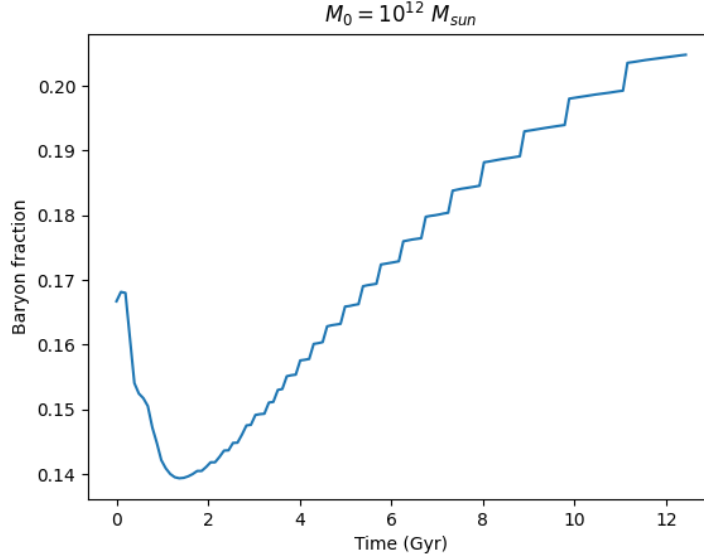


Figure 5: Evolution of baryon fraction over time.

In figure ??, I plot the evolution of the gas for different values of  $M_0$ .

In figure ??, I vary the value of  $\gamma$ .

## 2.1 Self-similarity and comparison

The x axis is normalized with respect to the virial radius  $R_{200c}$  at the present time ( $z=0$ ), while the density is normalized with respect to  $\rho_0 = M_{200}/R_{200c}^3$ , with  $M_{200}$  being the virial mass at  $z = 0$ .

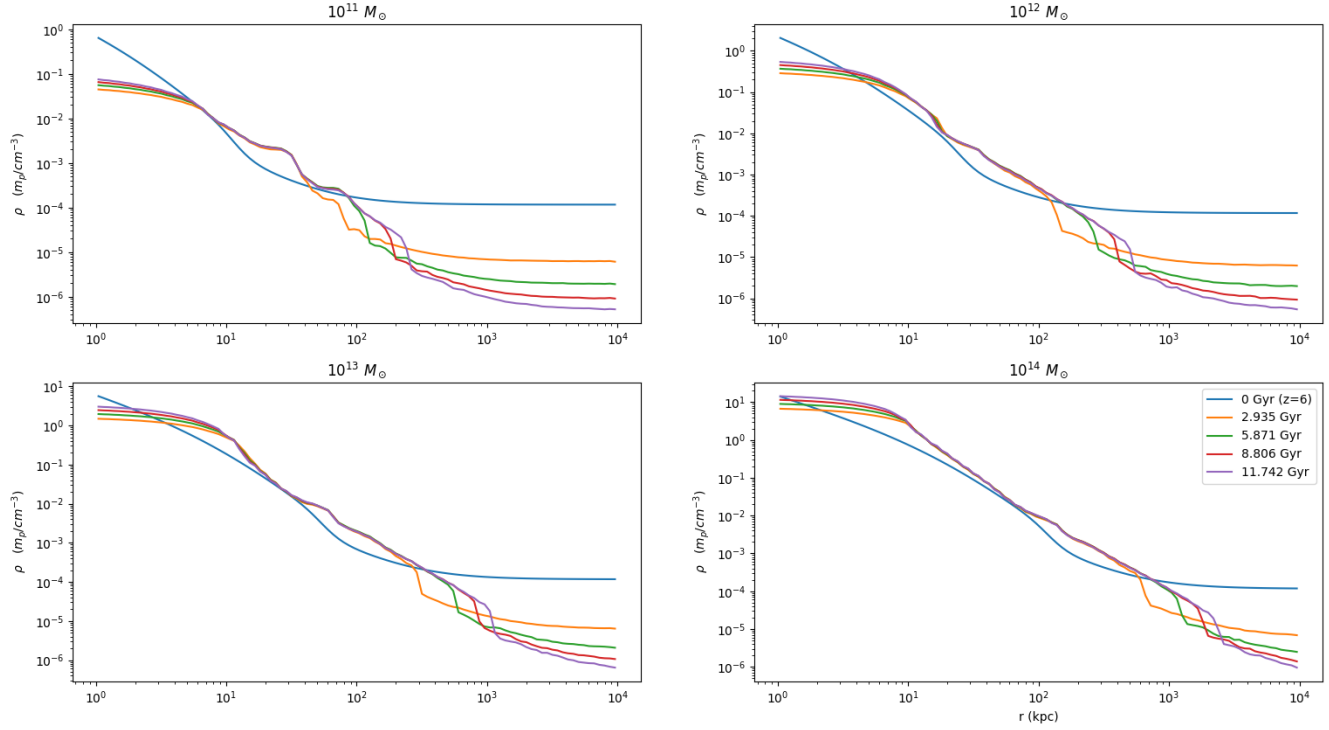


Figure 6: Different values of  $M_0$ .

In figure ??, I plot the normalized density vs normalized radius for different values of  $M_0$  at  $z=0$ .

In figure ??, I plot the same for different values of  $\gamma$ .

Next, I plot the value of the density power law index,  $d \log(\rho)/d \log(r)$  as a function of  $r$ .

Finally, I plot the value of  $\rho_g/\rho_{DM}$  as a function of  $r$ .

From the results, the following conclusions can be made:

- The density profiles are self-similar with respect to the current ( $z=0$ ) virial density and radius.
- The virial shock appears at a radius about 2 times the virial radius ( $R_{200c}$ ). This is in contradiction to the results from PPC, we have to investigate whether this is due to the difference in choice of potential, or if our simulations are wrong.
- The virial shock moves away from  $R_{200c}$  as the value of  $\gamma$  is increased.
- The baryon fraction and the value of  $\rho_g/\rho_{DM}$  deviate greatly from their expected values. We have to investigate why this is so.

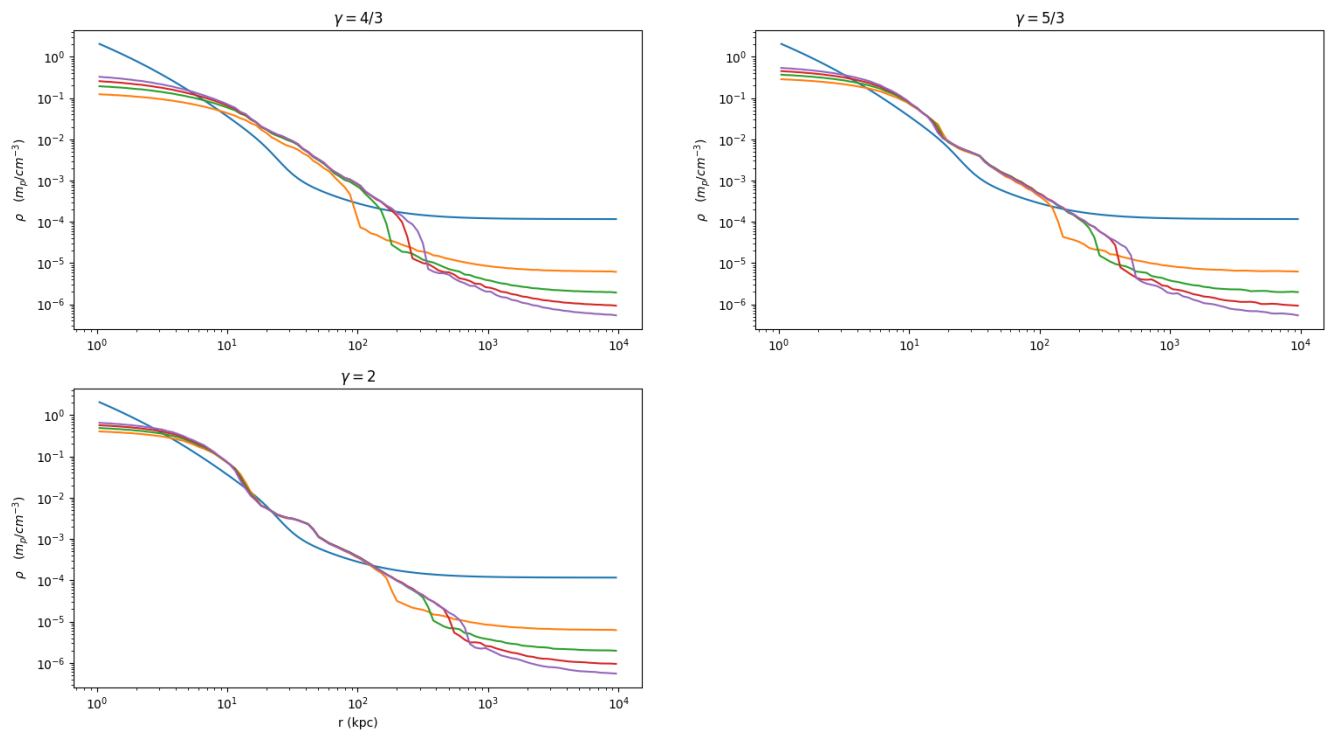


Figure 7: Different values of  $\gamma$ .

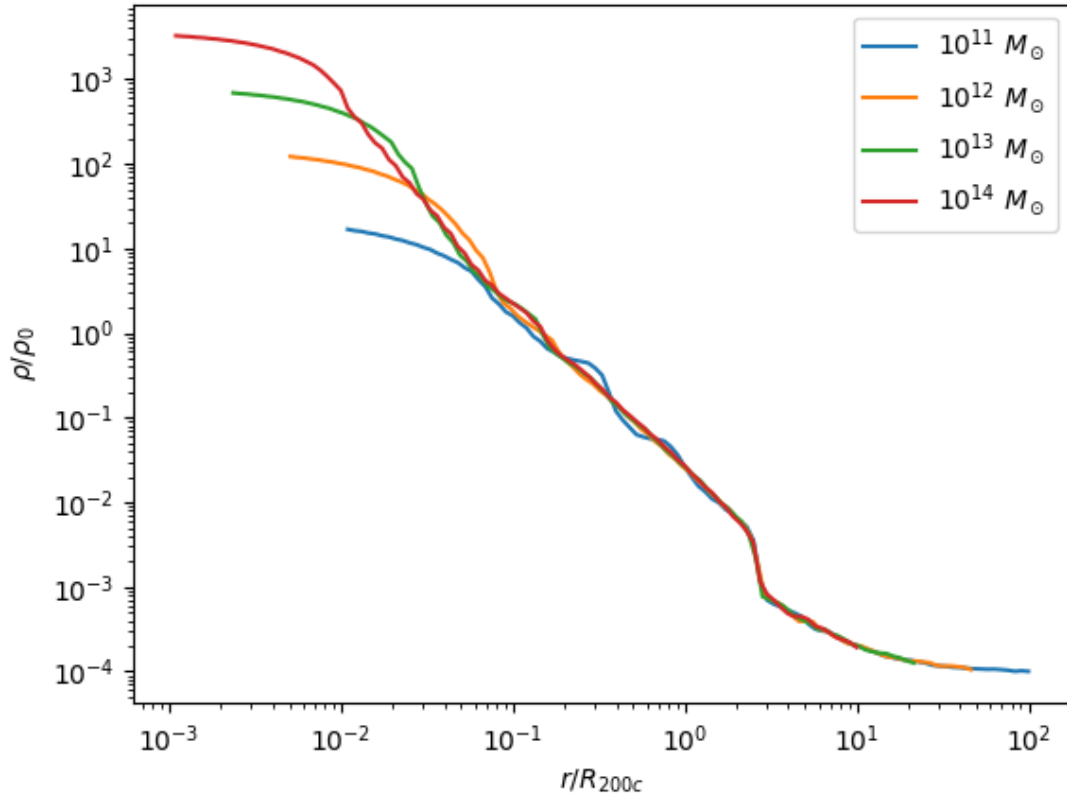


Figure 8: Self similar profiles at  $z = 0$  of  $\rho$  vs  $r$  for different  $M_0$ .



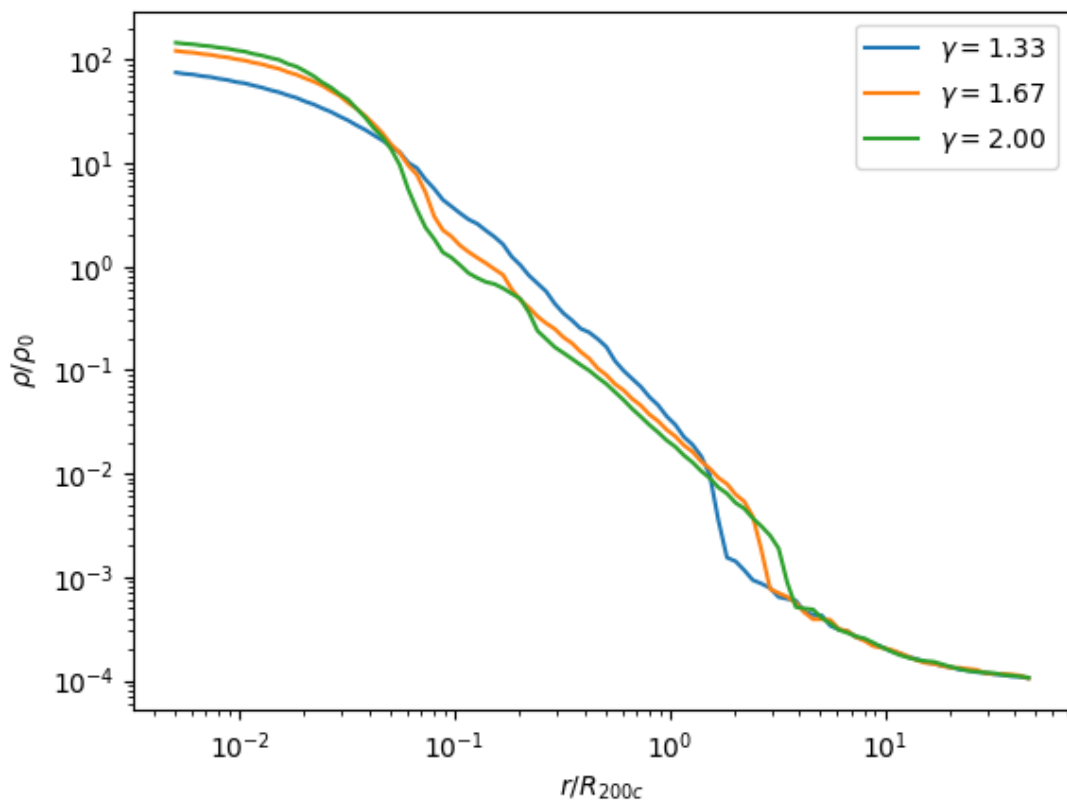


Figure 9: Self similar profiles at  $z = 0$  of  $\rho$  vs  $r$  for different  $\gamma$ .

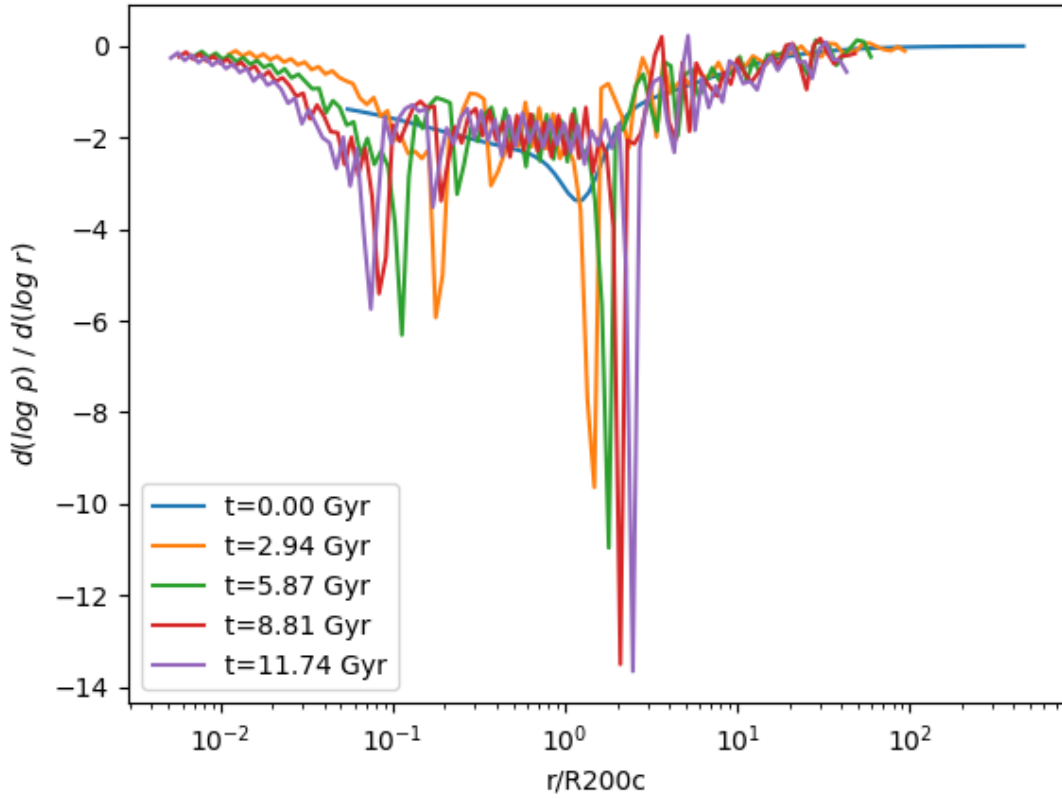


Figure 10: Power law index variation over  $r$ .  $M_0 = 10^{12} M_\odot$ .

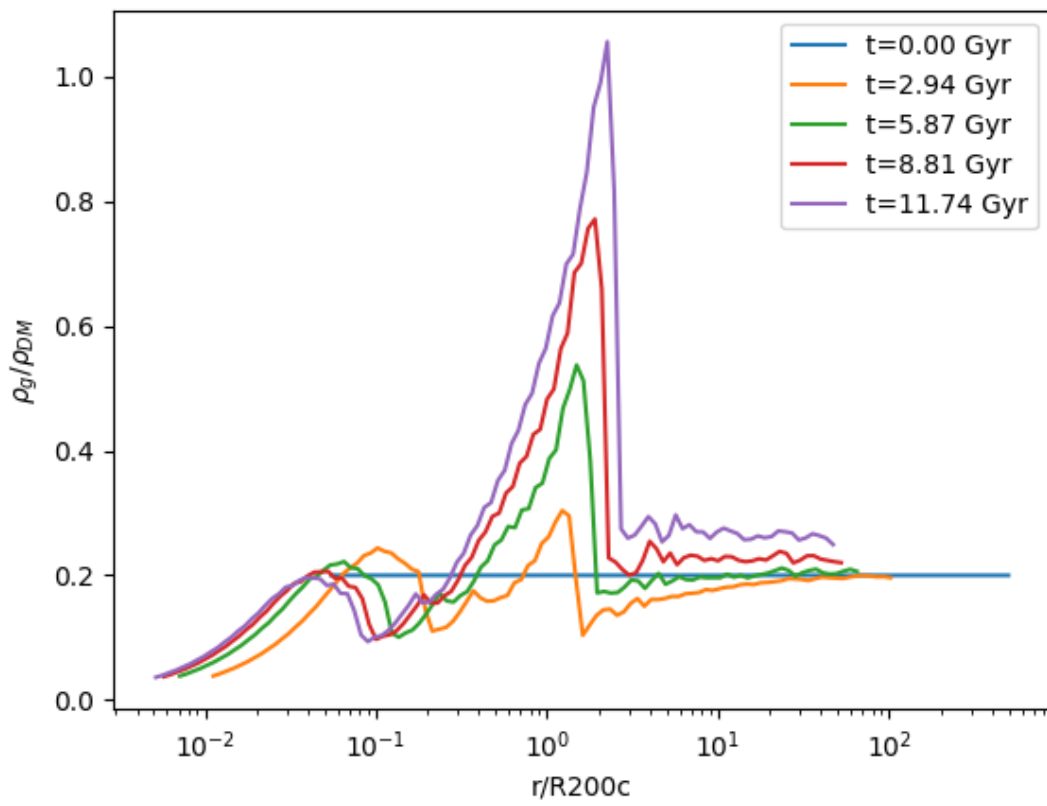


Figure 11:  $\rho_g/\rho_{DM}$  for  $M_0 = 10^{12} M_{\odot}$ .